OPTIMAL SYNTHESIS OF CIRCULAR APERTURES BASED ON LUDWIG DISTRIBUTIONS

J. C. Brégains, J. A. Rodríguez, F. Ares, and E. Moreno

Grupo de Sistemas Radiantes, Departamento de Física Aplicada,

Facultad de Física, Universidad de Santiago de Compostela.

15782 - Santiago de Compostela – Spain

faares@usc.es

ABSTRACT

Ludwig distributions are a generalization of circular Taylor distributions that generate radiation patterns with wide-angle side lobe levels decaying faster than for Taylor patterns. In this paper we show that by means of an appropriate optimization technique the zeros of Ludwig patterns can be perturbed so as to improve or modify pattern and/or aperture distribution characteristics without altering the wide-angle decay behaviour. The examples presented include footprint patterns, pencil beam patterns with individually controlled side lobe heights, footprint beams generated by real excitations, and pencil beam patterns with aperture distributions that are smoother than the original Ludwig distribution.

1. INTRODUCTION

For a circular antenna aperture of radius a with real axisymmetric excitation, T.T. Taylor [1] showed that if the excitation amplitude at the edge is proportional to $(1 - p^2)^{\alpha}$, where $p = r/a$ (r being distance from the centre of the aperture), then the wide-angle side lobes of the radia-

tion pattern decay as $u^{-(\alpha + 3/2)}$, where $u = (2a/\lambda)\sin\theta$ (λ being the wavelength and θ the angle from the zenith). The distributions bearing his name, which were designed to minimize the beamwidth given a specified maximum side lobe level *SLL*, correspond to the case $\alpha = 0$. Rhodes [2] showed that the $\alpha = 0$ case is in fact physically impossible (though approximable arbitrarily closely), and Ludwig [3] generalized Taylor's derivation of his distributions for $\alpha > 0$, and explored the performance of the resulting distributions for the simplest case, $\alpha = 1$. These "first-order generalized Taylor distributions", or Ludwig distributions, h_L, are obtained by integrating an expression for their derivative while imposing the boundary condition $h_L(1) = 0$:

$$h_L(p) = \int_1^p h_L'(\rho)d\rho \tag{1}$$

where

$$h_L'(\rho) = -8\rho + 8\sum_{i=1}^{\bar{n}-1} \frac{J_1(\gamma_{2i}\rho)}{J_1(\gamma_{2i})} \frac{\prod_{n=1}^{\bar{n}-1}\left(1 - \frac{\gamma_{2i}^2}{u_{Ln}^2}\right)}{\prod_{\substack{n=1 \\ n\neq i}}^{\bar{n}-1}\left(1 - \frac{\gamma_{2i}^2}{\gamma_{2n}^2}\right)} \tag{2}$$

J_1 being the first-order Bessel function of the first kind and γ_{2i} the *i*-th zero of the second-order Bessel function of the first kind (J_2), and the u_{Ln} being given by

$$u_{Ln} = \gamma_{2\bar{n}}\left[\frac{A^2 + \pi^2(n - \frac{1}{2})^2}{A^2 + \pi^2(\bar{n} - \frac{1}{2})^2}\right]^2 \tag{3}$$

where $A = \cosh^{-1}(10^{-SLL/20})$. The u_{Ln} are in fact the first $\bar{n}$ -1 zeros of the radiation pattern $F_L(u)$, given by [3]:

$$F_L(u) = 8\frac{J_2(u)}{u^2}\frac{\prod_{n=1}^{\bar{n}-1}\left(1-\frac{u^2}{u_{Ln}^2}\right)}{\prod_{n=1}^{\bar{n}-1}\left(1-\frac{u^2}{\gamma_{2n}^2}\right)} \tag{4}$$

In previous papers Elliott and Stern [4,5] and Ares and Rodríguez [6] have shown that, by using Taylor patterns as the starting points of appropriate optimization procedures, it is possible to achieve axisymmetric footprint patterns [4], axisymmetric footprint patterns and non-trivial side lobe topology from real excitations [5], and aperture distributions that are smoother than the corresponding Taylor distribution [6]. Here we report that application of the same approach to Ludwig distributions can achieve similar results.

2. METHOD

To achieve all the objectives mentioned above, it is necessary to generalize eq. 4:

$$F(u) = 8\frac{J_2(u)}{u^2}\frac{\prod_{n=1}^{M}\left(1-\frac{u^2}{(u_n+jv_n)^2}\right)\left(1-\frac{u^2}{(u_n-jv_n)^2}\right)^{\varepsilon}\prod_{n=M+1}^{\bar{n}-1}\left(1-\frac{u^2}{u_n^2}\right)}{\prod_{n=1}^{\bar{n}-1+\varepsilon M}\left(1-\frac{u^2}{\gamma_{2n}^2}\right)} \tag{5}$$

where the complex zeros achieve footprint beams by null filling; ε is 0 or 1 depending on whether the aperture distribution can be complex or must be real (in which case complex zeros have to be accompanied by their complex conjugates); and in each specific application the values of the u_n and v_n initialized to those of the appropriate Ludwig distribution (the v_n are of course initially zero), and are then optimized by successive perturbations so as to minimize a cost function C that penalizes the deviation of pattern and/or aperture distribution parameters from desired values. In the course of this optimization process the aperture distribution $h(p)$ is

calculated by eq.1 (with $h(p)$ instead of $h_L(p)$) using the appropriate generalization of eq.2:

$$h'(\rho) = -8\rho + 8\sum_{i=1}^{\bar{n}-1} \frac{J_1(\gamma_{2i}\rho)}{J_1(\gamma_{2i})} \frac{\prod_{n=1}^{M}\left(1-\frac{\gamma_{2i}^{\ 2}}{(u_n+jv_n)^2}\right)\left(1-\frac{\gamma_{2i}^{\ 2}}{(u_n-jv_n)^2}\right)^{\varepsilon}\prod_{n=M+1}^{\bar{n}-1}\left(1-\frac{\gamma_{2i}^{\ 2}}{u_n^2}\right)}{\prod_{\substack{n=1\\ n\neq i}}^{\bar{n}-1+\varepsilon M}\left(1-\frac{\gamma_{2i}^{\ 2}}{\gamma_{2n}^2}\right)} \tag{6}$$

3. EXAMPLES

In this section we exemplify the potential of the above approach by synthesizing excitation distributions complying with a variety of pattern or aperture distribution requirements. All these examples concern an aperture of radius $a = 5\lambda$, and in all cases the optimization technique employed was simulated annealing [7].

3.1. A pencil beam with a "moat"

If the desired level of the first side lobe around a pencil beam ($SLL_{1,d}$) is -40 dB, and no other is to exceed -20 dB, then we take $\bar{n}$ large enough to give good directivity, set the desired level $SLL_{i,d}$ to -20 dB for side lobes 2 to $\bar{n}-1$, (set M=0 in eqs.5 and 6) and optimize the cost function

$$C = \sum_{i=1}^{\bar{n}-1}(SLL_i - SLL_{i,d})^2 \tag{7}$$

For $\bar{n} = 5$, the pattern so obtained is shown in Fig.1, and its nulls u_n are listed in Table 1. Its peak directivity D_0, calculated as

$$D_0 = \frac{1}{\int_0^{\pi/2} |F(\theta)|^2 \sin\theta d\theta} = \frac{(2\pi a/\lambda)^2}{\int_0^{2\pi a/\lambda} \frac{|F(u)|^2 \, du}{\sqrt{1-\left(\frac{u}{2\pi a/\lambda}\right)^2}}} \tag{8}$$

is 530, and where |F(θ)| is the modulus of the normalized pattern function. The excitation amplitude distribution is shown in Fig.2 (the phase is of course zero for this pattern). Note that, since only the side lobe levels have been controlled in the optimization process, the price paid for good directivity is a degree of irregularity in aperture distribution. The amelioration of this undesirable behaviour is discussed below in Section 3.4.

3.2. A flat-topped beam with controlled side lobes

If we wish to obtain a flat-topped beam by filling the first M nulls to Δz dB below the beam top, and at the same time ensure that the first r side lobes do not exceed a desired level SLL_d, then we take $\bar{n} = M + r + 1$, $SLL_{1,d} = ... = SLL_{M,d} = 0$ dB, $SLL_{M+1,d} = ... = SLL_{\bar{n}-1,d} = SLL_d$ dB and $\varepsilon = 0$ (we do not demand that the aperture distribution be real), and we optimize the cost function

$$C = \sum_{i=1}^{\bar{n}-1} (SLL_i - SLL_{i,d})^2 + \sum_{i=1}^{M} (Z_i - Z_d)^2 \tag{9}$$

where Z_i is the power level at filled null i (i.e. at $u = u_i$ for $i = 1,...,M$) and $Z_d = -\Delta z$ dB. For $M = 2$, $r = 3$, $\Delta z = 1$ and $SLL_d = -20$ dB, the pattern and distribution results are shown in Figs.3-5 and the values of the u_n and v_n are listed in Table 2.

3.3. A flat-topped beam with controlled side lobes generated by a real aperture excitation

If we perform the same optimization as in Section 3.2, but with ε = 1 so as to achieve a real aperture distribution, then we obtain the pattern shown in Fig.6 (its zeros are listed in Table 3) and the aperture distribution shown in Fig.7. The price paid for ensuring that the excitation is real by making consecutive filled zeros mutual conjugates is a significant broadening of the main beam.

3.4. Pencil beams generated by smooth aperture distributions

A pattern that satisfies the same specifications as for the pattern of Section 3.1 can be achieved using a smoother aperture distribution than in Section 3.1 if null-filling and a complex excitation are allowed ($M = \bar{n} - 1$, $\varepsilon = 0$ in eqs. 5 and 6) and the cost function of eq.8 is supplemented with *a*) a term preventing the levels of the filled nulls from becoming too close to the adjacent side lobe levels, and *b*) a term limiting the local variation of the excitation amplitude distribution:

$$C = c_1 \sum_{i=1}^{\bar{n}-1} (SLL_i - SLL_{i,\mathrm{d}})^2 + c_2 \sum_{i=1}^{q} (Z_i - Z_{i,\mathrm{d}})^2 + c_3 (V - V_{\mathrm{d}})^2 \qquad (10)$$

where the $Z_{i,\mathrm{d}}$ are the desired maximum null filling levels; $q = 2$ if $Z_i < Z_{i,\mathrm{d}}$ for $2 < i \le \bar{n} - 1$ and $q = \bar{n} - 1$ otherwise (this forces Z_1 and Z_2 to adopt the desired values, but allows the other controlled nulls to be filled to levels below the specified maximum level); $V = \max\{R_j\}$, where R_j is the difference between the j-th peak of the excitation amplitude distribution and the lower of its flanking minima; V_{d} is the desired value of V; and the c_i are adjustable constants controlling the relative importance of fixing side lobe levels, null-filling levels and the

local variation of the aperture amplitude distribution.

The radiation pattern and aperture distribution obtained for the same $\bar{n}$ and $SLL_{i,\mathrm{d}}$ as in Section 3.1, $Z_{1,\mathrm{d}} = Z_{2,\mathrm{d}} = -41$ dB, $Z_{3,\mathrm{d}} = Z_{4,\mathrm{d}} = -21$ dB and $V_{\mathrm{d}} = 0.05$ are shown as continuous curves in Figs. 8-10 (with the corresponding functions of Section 3.1 shown as dashed curves for comparison), and the u_n and v_n are listed in Table 4. The price paid for making the aperture amplitude distribution smoother (edge-brightening has virtually disappeared) is just a 5.5% reduction in directivity from 530 to 501.

3.5. Ludwig patterns without edge-brightening

Finally, we apply our methodology to making the aperture distributions for Ludwig patterns smoother without raising the side lobe levels of the patterns themselves or significantly reducing their peak directivities. For a Ludwig pattern with $\bar{n} = 8$ and a side lobe level of -25 dB (M=0, $SLL_{i,\mathrm{d}} = -25$ dB), we use the cost function

$$C = c_1 \sum_{i=1}^{7} \Delta_i^2 H(\Delta_i) + c_2 (D_0 - D_{\mathrm{d}})^2 + c_3 (V - V_{\mathrm{d}})^2 \qquad (11)$$

where D_{d} is the desired peak directivity (that of the original Rhodes pattern, in this case 538), $\Delta_i = (SLL_i - SLL_{i,\mathrm{d}})$, and H is the Heaviside step function. The continuous curves in Figs.11 and 12 show the results obtained setting $V_{\mathrm{d}} = 0.05$, and the dashed curves those of the original Ludwig distribution. Note that the aperture distribution is now monotonic, so that edge-brightening has been totally eliminated. The price paid for this is a slight (3.4%) reduction in peak directivity (now 520). The values of u_n are listed for both patterns in Table 5.

4. FINAL REMARKS

The above examples show that by means of an appropriate optimization technique the zeros of Ludwig radiation patterns can be perturbed so as to improve or modify the characteristics of the pattern and/or the aperture distribution without altering the decay behaviour of the wide-angle side lobes. In this way it is possible to achieve footprint patterns with individually controlled inner side lobe heights, and pencil beams with aperture distributions that are smoother than the original Ludwig distribution, using either real or complex excitations. The syntheses presented here, in which optimization was performed by simulated annealing, took between 10 seconds and 5 minutes on a PC with an AMD-K6-2 processor running at 500 MHz.

The present results can be implemented using planar array antennas with circular boundaries by sampling the aperture distributions described in this paper (after which the array can be further optimized by means of techniques appropriate to discrete arrays). The method described here is also generalizable to the synthesis of distributions for blocked apertures, in a way analogous to the method developed by Ludwig [3].

ACKNOWLEDGEMENT

This work was supported by the Spanish Ministry of Science and Technology under project TIC2000-0401-P4-09.

REFERENCES

[1] Taylor, T.T.. 1960. Design of circular apertures for narrow beamwidth and low side lobes, *Trans. IRE.* AP-8: 17-22.

[2] Rhodes, D.R.. 1972. On the Taylor distribution. *IEEE Trans. Antennas Propagat.* AP-20 (2): 143-145.

[3] Ludwig, A.C.. 1982. Low sidelobe aperture distributions for blocked and unblocked circular apertures. *IEEE Trans. on Antennas and Propagat.*, AP-30 (5): 933-946.

[4] Elliott, R.S. & G. J. Stern. 1988. Shaped patterns from a continuous planar aperture distribution, *IEEE Proceedings*, 135 Pt. H (6): 366-370.

[5] Elliott, R.S. & G. J. Stern. 1990. Footprint patterns obtained by planar arrays. *IEEE Proceedings*, 137 Pt.H (2): 108-112.

[6] Ares, F. & J. A. Rodríguez. 1998. Smooth, efficient real amplitude distributions with no edge brightening for linear and circular near-Taylor sum patterns. *Electronics Letters*, 34 (7): 611-612.

[7] Press, W.H., S. A. Teukolsky, W. T. Vetterling, & B. P. Flannery, *Numerical Recipes in C,* Cambridge University Press: 444-455.

LEGENDS FOR FIGURES AND TABLES

- **Fig.1.** The pencil beam pattern obtained in Section 3.1.
- **Fig.2.** Amplitude of the aperture distribution affording the radiation pattern of Fig.1.
- **Fig.3.** Footprint beam obtained in Section 3.2. Ripple, ± 0.5 dB; side lobe level, -20 dB.
- **Fig.4.** Amplitude of the aperture distribution affording the radiation pattern of Fig.3.
- **Fig.5.** Phase of the aperture distribution affording the radiation pattern of Fig.3.
- **Fig.6.** Flat-topped beam obtained in Section 3.3 using a real aperture distribution. Ripple, ± 0.5 dB; side lobe level, -20 dB.
- **Fig.7.** Amplitude of the aperture distribution affording the radiation pattern of Fig.6.
- **Fig.8.** Pencil beam pattern obtained in Section 3.4 while minimizing the variation of the aperture distribution (———), and the pattern obtained in Section 3.1 without aperture optimization (----).
- **Fig.9.** Amplitudes of the aperture distributions affording the radiation patterns of Fig.8. Note the reduction in edge-brightening.
- **Fig.10.** Phase of the aperture distribution affording the smoother radiation pattern of Fig.8.
- **Fig.11.** Pencil beam pattern similar to a Ludwig pattern obtained with a smooth aperture distribution in Section 3.5 (———), and the original -25 dB $\bar{n} = 8$ Ludwig pattern used as starting point.
- **Fig.12.** Amplitudes of the aperture distributions affording the radiation patterns of Fig.11. Note the total elimination of edge-brightening.
- **Table 1.** Zeros of the radiation pattern of Fig.1 (Section 3.1).
- **Table 2.** Zeros of the radiation pattern of Fig.3 (Section 3.2).

- **Table 3.** Zeros of the radiation pattern of Fig.6 (Section 3.3).
- **Table 4.** Zeros of the radiation pattern of Fig.8 (Section 3.4).
- **Table 5.** Zeros of the radiation pattern of Fig.11 (Section 3.5).

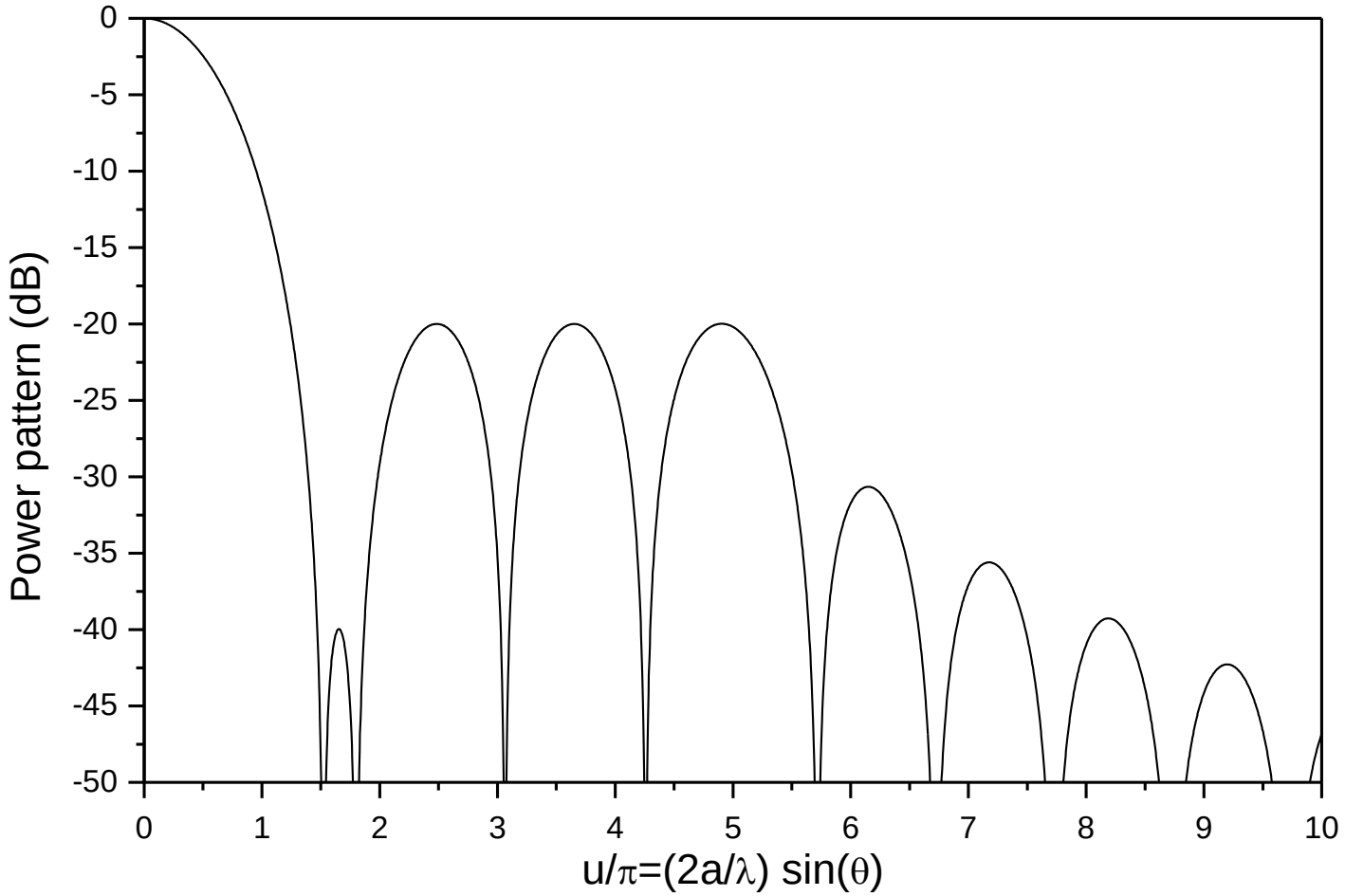
0
-5
-10
-15
-20
-25
-30
-35
-40
-45
-50
Power pattern (dB)
0
1
2
3
4
5
6
7
8
9
10
u/π=(2a/λ) sin(θ)

Fig. 1

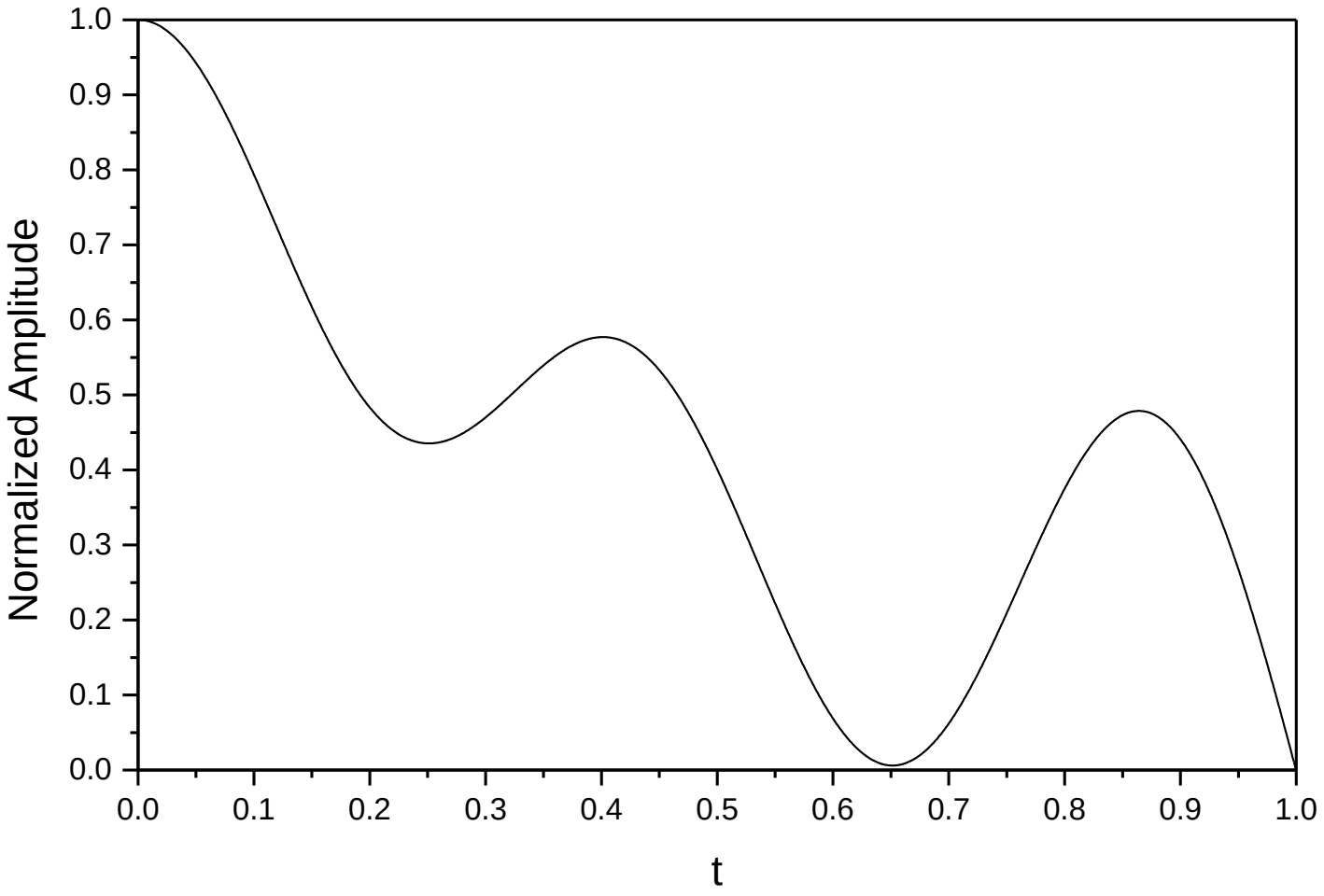
Normalized Amplitude
1.0
0.9
0.8
0.7
0.6
0.5
0.4
0.3
0.2
0.1
0.0
0.0
0.1
0.2
0.3
0.4
0.5
0.6
0.7
0.8
0.9
1.0
t

Fig. 2

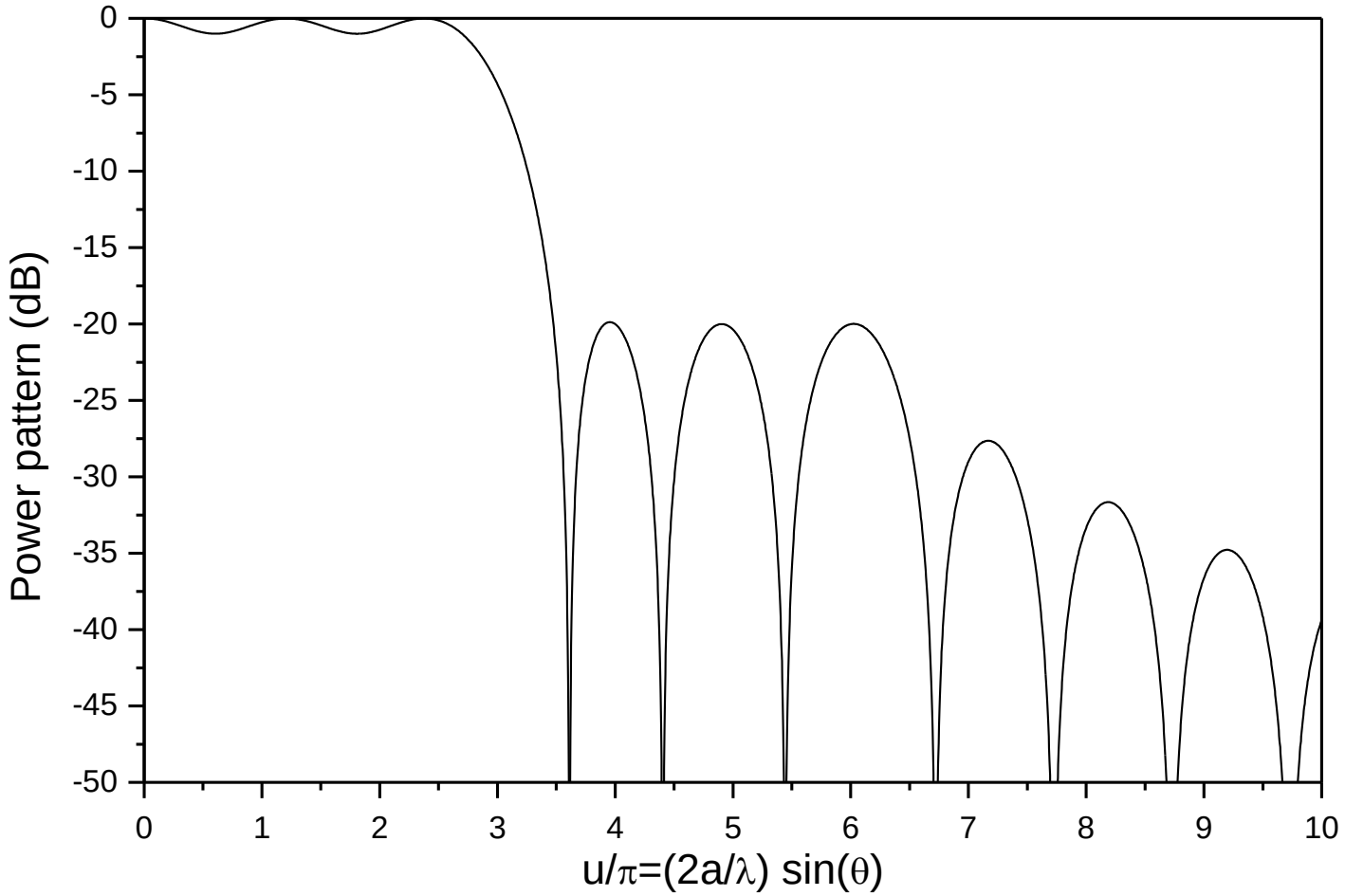
0
-5
-10
-15
-20
-25
-30
-35
-40
-45
-50
Power pattern (dB)
0
1
2
3
4
5
6
7
8
9
10
u/π=(2a/λ) sin(θ)

Fig. 3

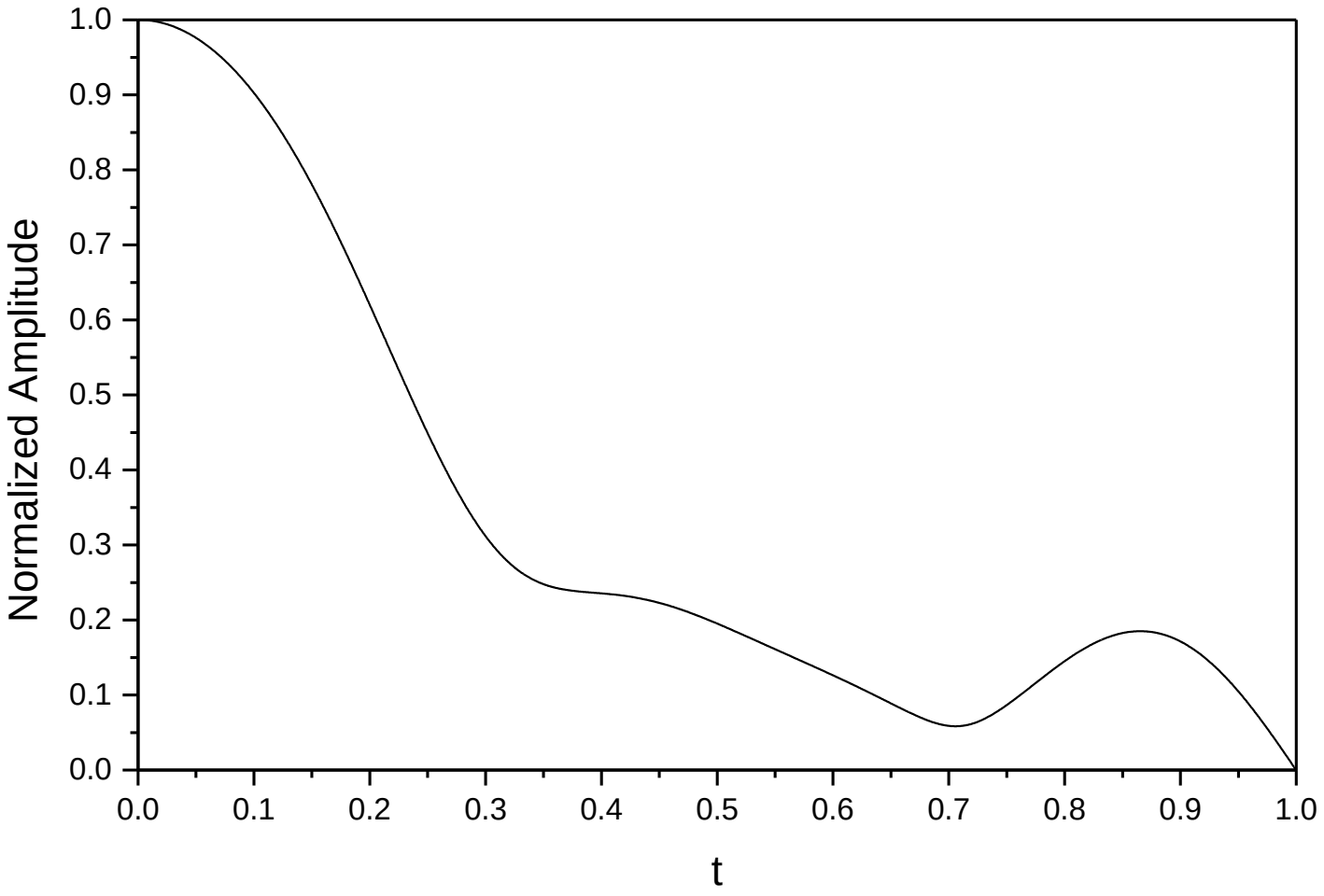
Normalized Amplitude
1.0
0.9
0.8
0.7
0.6
0.5
0.4
0.3
0.2
0.1
0.0
0.0
0.1
0.2
0.3
0.4
0.5
0.6
0.7
0.8
0.9
1.0
t

Fig. 4

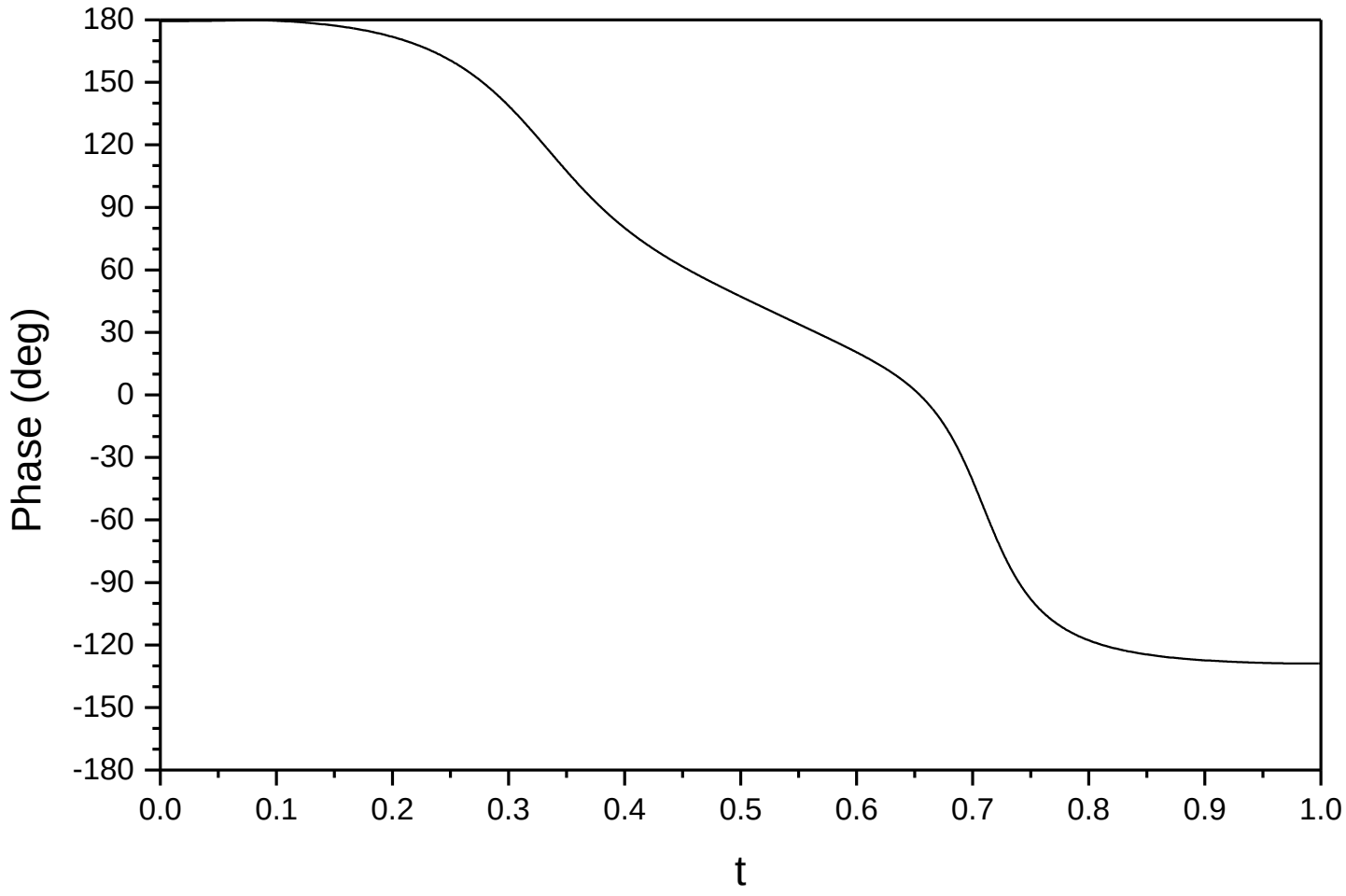
Phase (deg)
180
150
120
90
60
30
0
-30
-60
-90
-120
-150
-180
0.0
0.1
0.2
0.3
0.4
0.5
0.6
0.7
0.8
0.9
1.0
t

Fig. 5

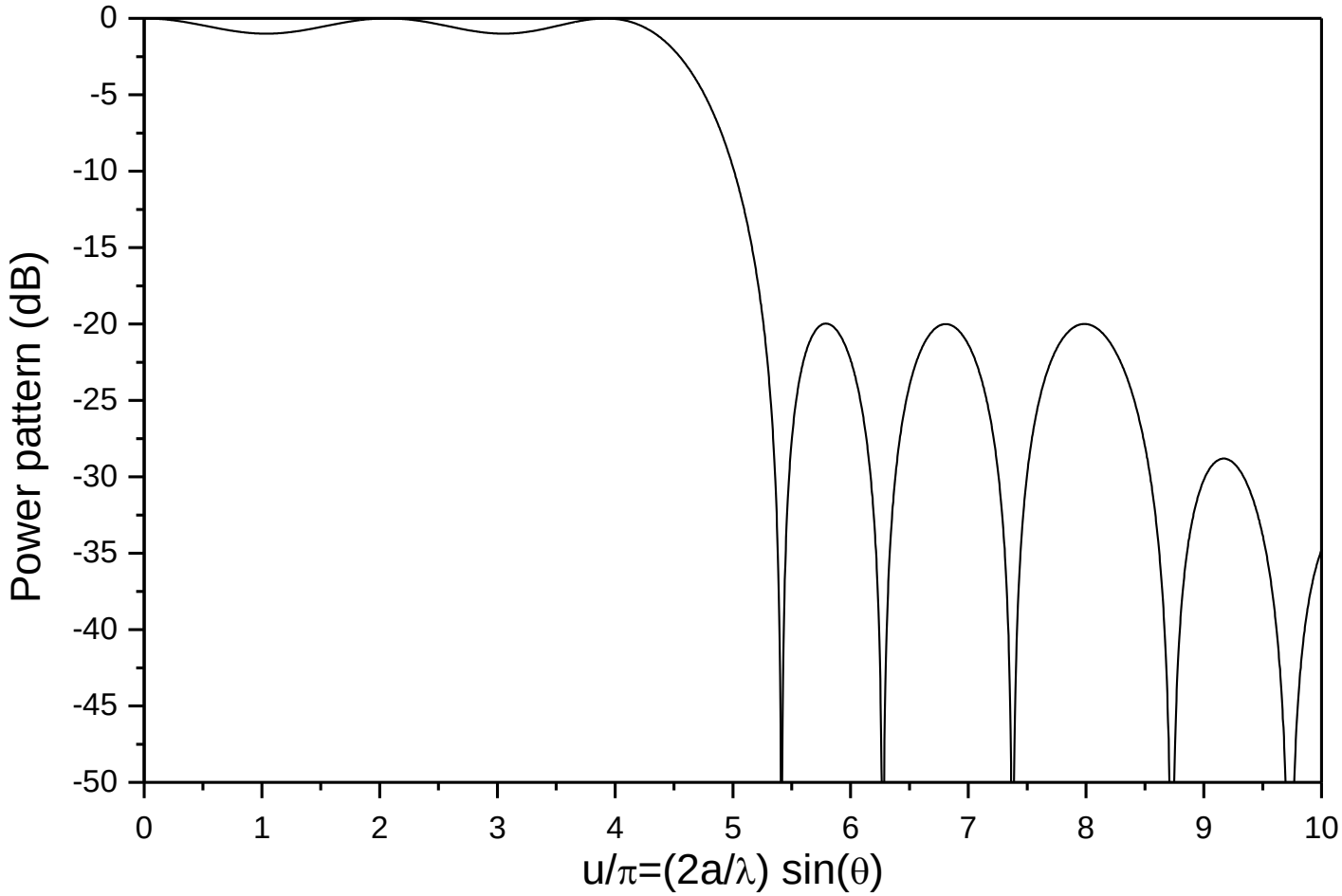
Power pattern (dB)
0
-5
-10
-15
-20
-25
-30
-35
-40
-45
-50
0
1
2
3
4
5
6
7
8
9
10
u/π=(2a/λ) sin(θ)

Fig. 6

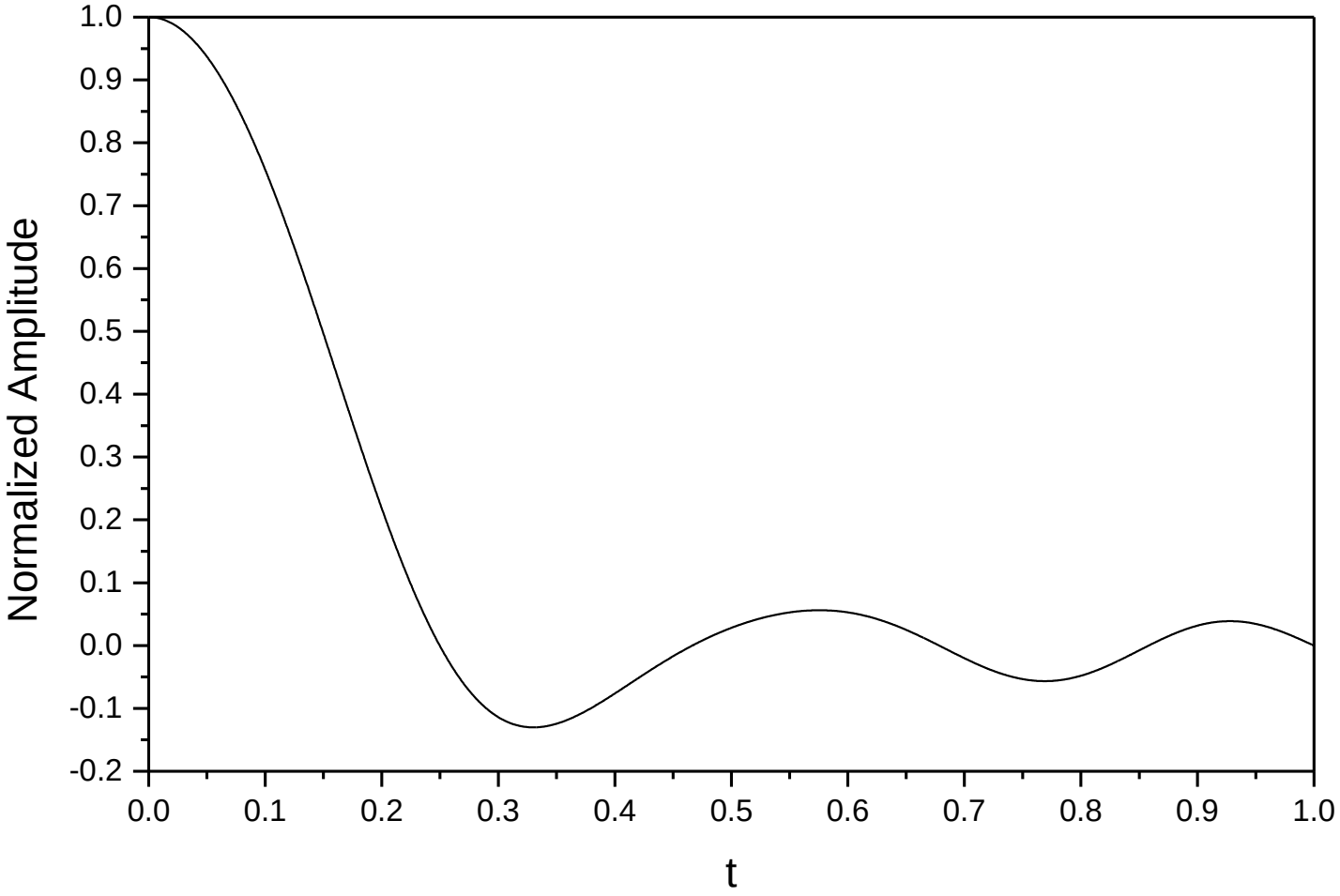
Normalized Amplitude
1.0
0.9
0.8
0.7
0.6
0.5
0.4
0.3
0.2
0.1
0.0
-0.1
-0.2
0.0
0.1
0.2
0.3
0.4
0.5
0.6
0.7
0.8
0.9
1.0
t

Fig. 7

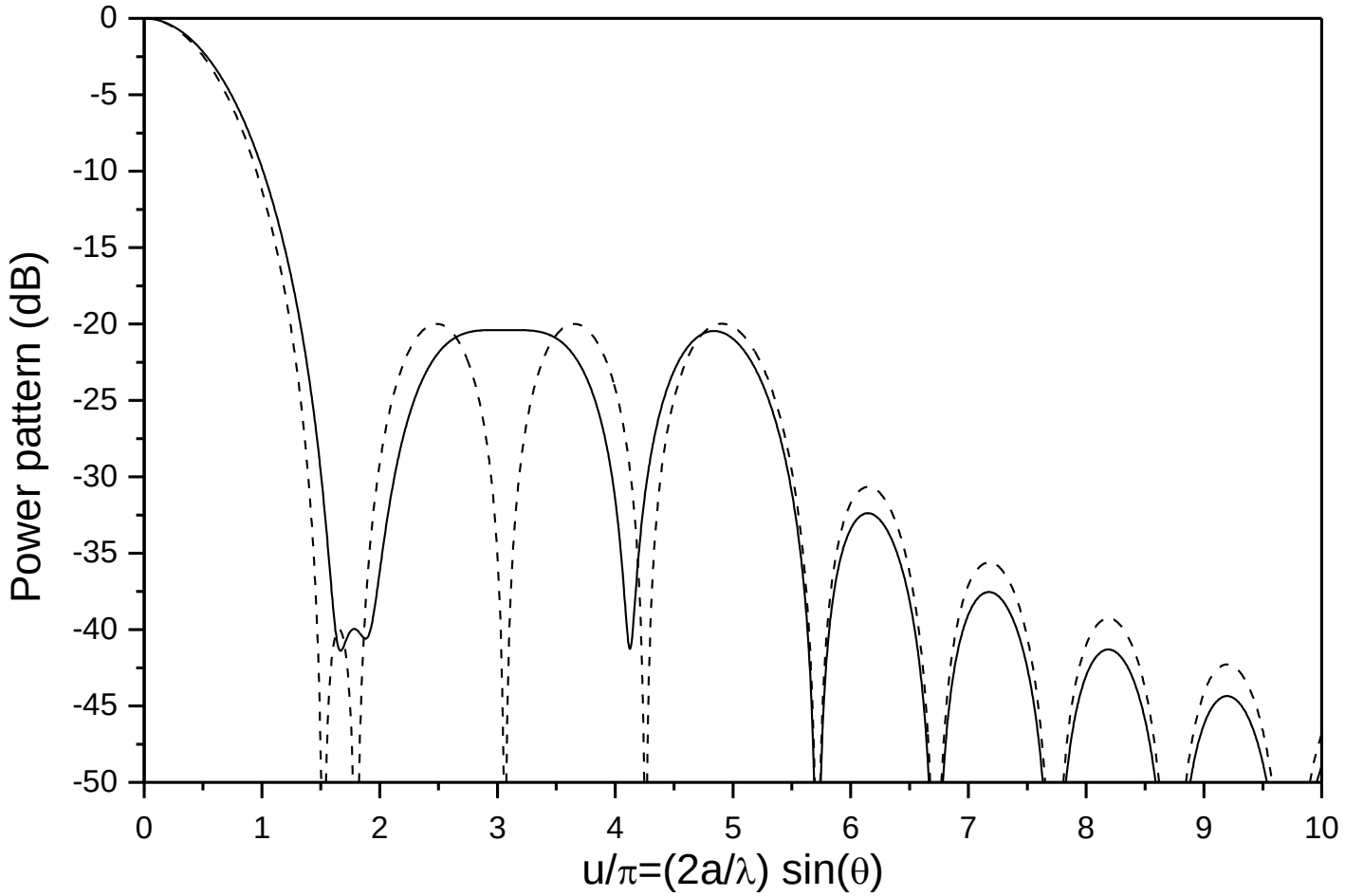
0
-5
-10
-15
-20
-25
-30
-35
-40
-45
-50
Power pattern (dB)
0
1
2
3
4
5
6
7
8
9
10
u/π=(2a/λ) sin(θ)

Fig. 8

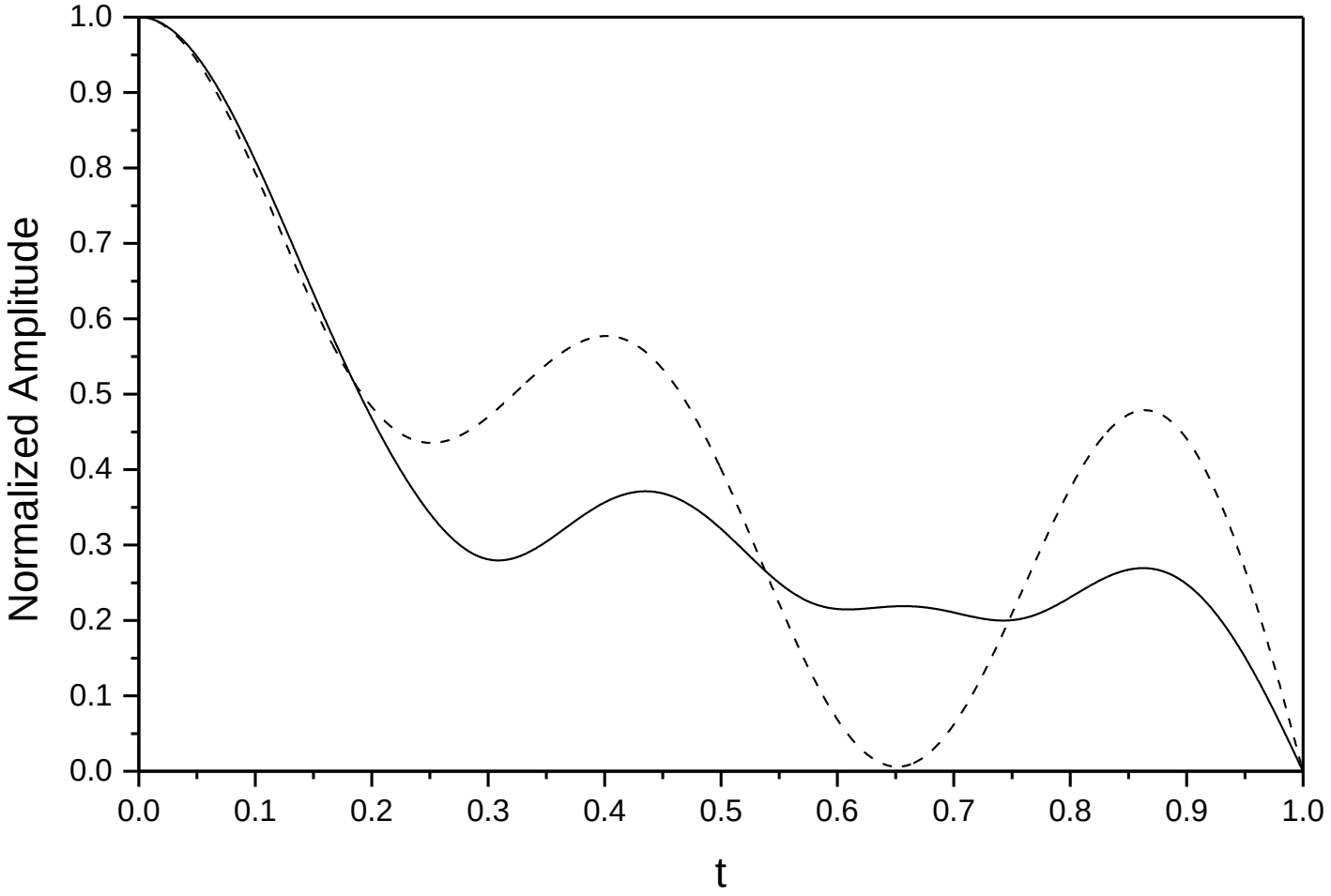
Normalized Amplitude
t
1.0
0.9
0.8
0.7
0.6
0.5
0.4
0.3
0.2
0.1
0.0
0.0
0.1
0.2
0.3
0.4
0.5
0.6
0.7
0.8
0.9
1.0

Fig. 9

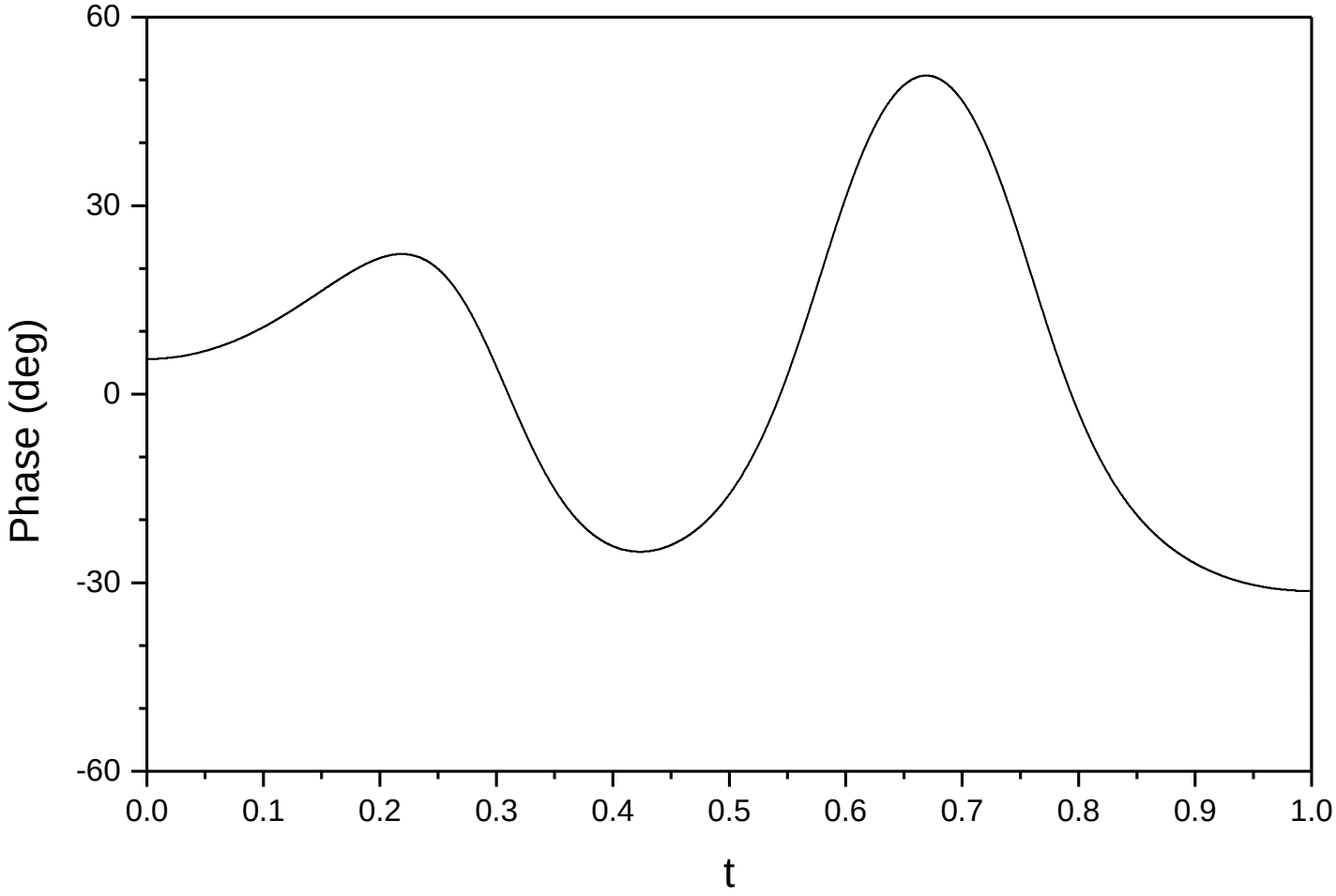

Fig. 10

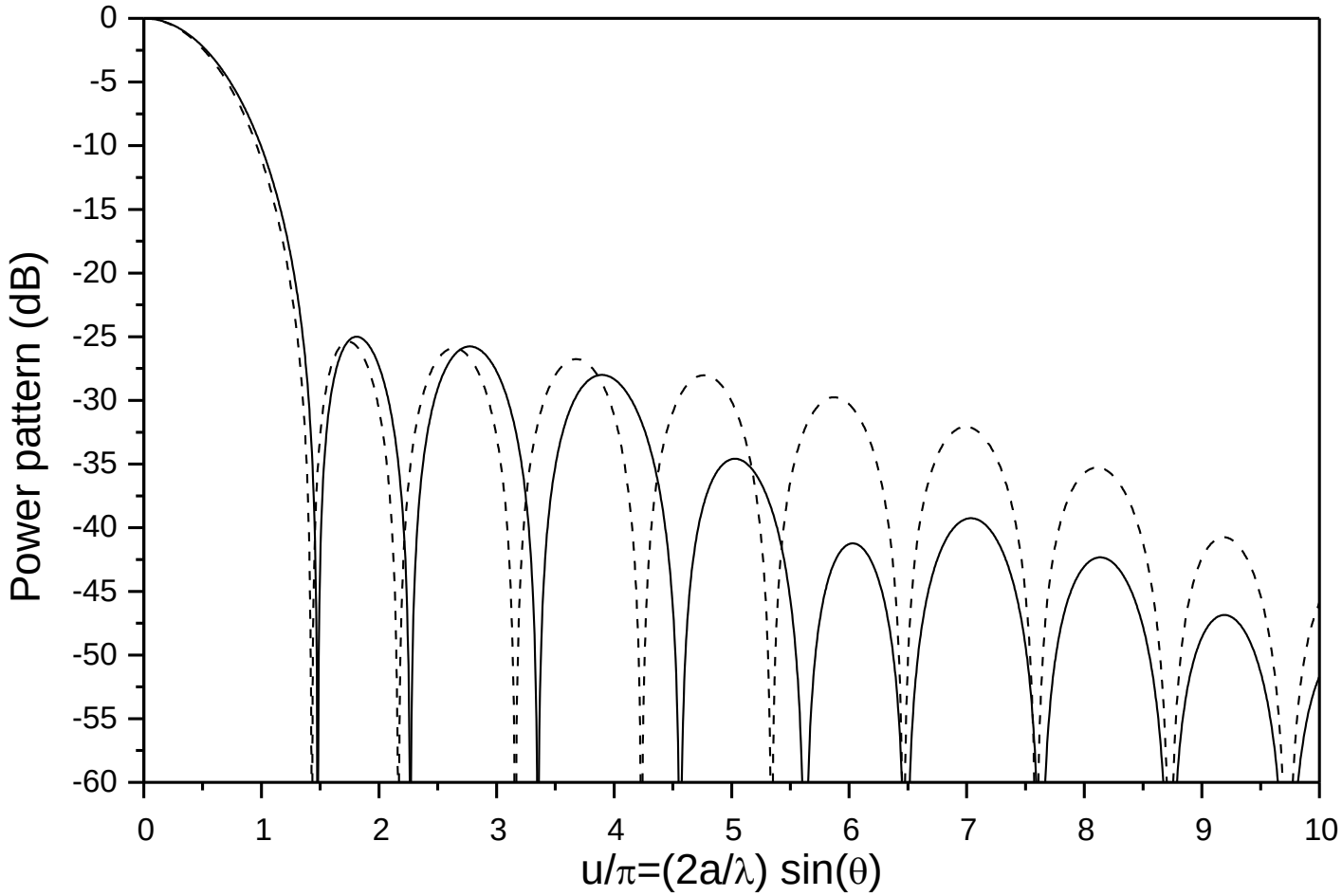
Power pattern (dB)
0
-5
-10
-15
-20
-25
-30
-35
-40
-45
-50
-55
-60
0
1
2
3
4
5
6
7
8
9
10
u/π=(2a/λ) sin(θ)

Fig. 11

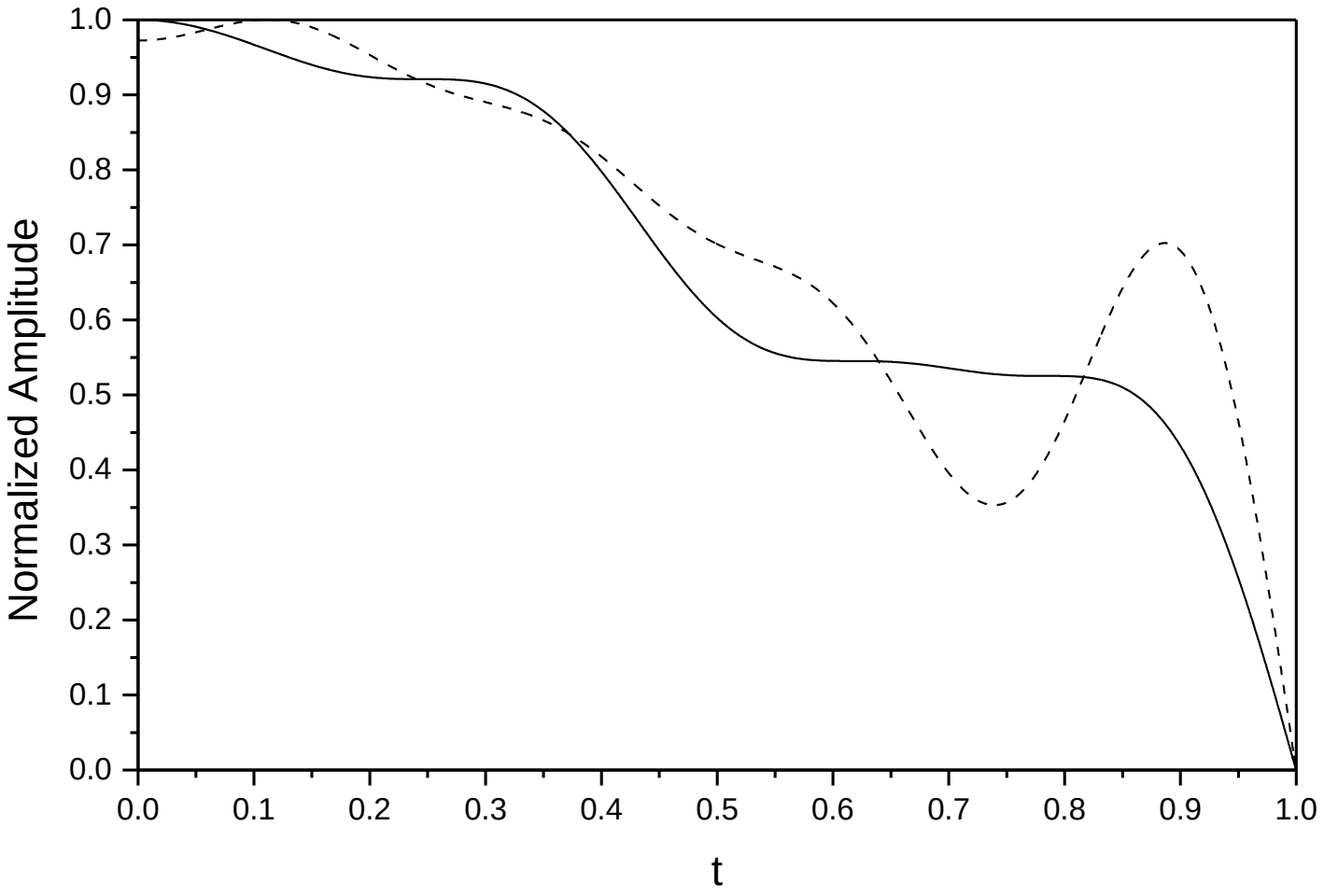
Normalized Amplitude
t
1.0
0.9
0.8
0.7
0.6
0.5
0.4
0.3
0.2
0.1
0.0
0.0
0.1
0.2
0.3
0.4
0.5
0.6
0.7
0.8
0.9
1.0

Fig. 12

Table 1

u_n
4.7795
5.6559
9.6274
13.3778

Table 2

u_n	v_n
1.8975	-1.7247
5.7029	1.7125
11.3459	0.0000
13.8356	0.0000
17.1019	0.0000

Table 3

u_n	v_n
3.2770	3.6763
9.7575	3.4658
17.0073	0.0000
19.7107	0.0000
23.1730	0.0000

Table 4

u_n	v_n
5.1642	0.2224
6.0060	0.3132
9.6276	1.8349
12.9594	-0.1311

Table 5

u_n	
Ludwig	**This work**
4.4884	4.6473
6.8029	7.1227
9.9271	10.5325
13.3022	14.3351
16.7774	17.6727
20.3015	20.3638
23.8527	23.9690